Engineering Science and Technology, an International Journal 20 (2017) 563–569

HOSTED BY

Contents lists available at ScienceDirect

Engineering Science and Technology, an International Journal

journal homepage: www.elsevier.com/locate/jestch

Full Length Article

Characterization and antibacterial activity of nickel ferrite doped α-*alumina* nanoparticle

Kariim Ishaq [a,*], Abdulkareem Ambali Saka [a,b], Abubakre Oladiran Kamardeen [a,c], Aliyu Ahmed [d], Mohammed Is'haq Alhassan [b], Hamidu Abdullahi [e]

[a] *Nanotechnology Research Group, Centre for Genetic Engineering and Biotechnology (CGEB), Federal University of Technology, P.M.B 65, Bosso, Minna, Niger State, Nigeria*
[b] *Department of Chemical Engineering, School of Engineering and Engineering Technology, Federal University of Technology, P.M.B 65, Gidan Kwano, Minna, Niger State, Nigeria*
[c] *Department of Mechanical Engineering, School of Engineering and Engineering Technology, Federal University of Technology, P.M.B 65, Gidan Kwano, Minna, Niger State, Nigeria*
[d] *Department of Chemical Sciences, Federal University, P.M.B 1020, Wukari, Taraba State, Nigeria*
[e] *Department of Microbiology, School of Life Sciences, Federal University of Technology, P.M.B 65, Bosso, Minna, Niger State, Nigeria*

ARTICLE INFO

Article history:
Received 26 September 2016
Revised 12 December 2016
Accepted 15 December 2016
Available online 28 December 2016

Keywords:
Nickel ferrite
α-Alumina
Antibacterial
Central composite design

ABSTRACT

The magnetic behaviour towards biomedical applications of transition metal-ferrite and transition metal-ferrite based nanoparticles is dependent upon the nanoparticles preparation parameters. In this study, an experimental design using central composite design (CCD) has been explored in the production of alumina based nickel-ferrite nanoparticles via wet impregnation method. The effects of operating conditions such as drying temperature, drying time and mass of support on the percentage yield of nickel-ferrite were studied. The optimum nickel-ferrite yield of 97.45% was obtained at 7.5 g of α-alumina, drying time of 7 h and drying temperature of 116.70 °C and then characterized using SEM, EDS and XRD to determine the surface morphology, elemental analysis and crystallinity respectively. The antibacterial activities of the nickel-ferrites doped α-alumina were tested on Gram-negative bacterium: *E. coli* and *Pseudomonas aeruginosa* and a Gram-positive bacterium *S. aureus*. The antibacterial results of the nickel ferrites doped α-alumina nanoparticle on microorganisms showed that the nanoparticles shows no effect on the growth of *E. coli* but depicts an inhibitory growth on *Pseudomonas aeruginosa* and *S. aureus* with high antibacterial effect on *S. aureus* of 1.70 mm diameter of inhibition. Hence, the developed nickel ferrites doped α-alumina nanoparticle shows high antibacterial effect on *Pseudomonas aeruginosa* and *S. aureus* which makes it a potential material for biomedical application.

1. Introduction

Ternary metal oxides such as cobalt ferrite, nickel ferrite, cupric ferrite, and zinc ferrite are being extensively investigated for their biomedical applications due to their favourable ferromagnetic properties Suresh et al. [8]. Recently, several researches showed the antibacterial potentials of these metal-oxide systems. Numerous areas of applications of the Nano-ferrites have been identified in several technological fields, making it one of the major focuses of nanotechnology research in the last decade [9]. The various applications are as a result of the interesting and extraordinary characteristics of these ferrites which include their improved electronic, magnetic, optical as well as catalytic properties. On the area of ferrites as an excellent catalyst material, its high chemical stability enhances this property most especially in the area of carbon nanotubes production via catalytic vapour deposition (CVD) techniques [4].

The magnetic nanoferrites are generally represented as MFe_2O_4 where M represents either of Ni, Co, or Cu that are tetrahedral sites of typical bivalent cations in a cubic lattice structure [5]. Uniquely, the nanoferrites of nickel are known to possess distinctive properties of high permeability when subjected to an elevated frequency and electrical resistivity. This exceptional property of nickel ferrite in the group of cubic ferromagnetic oxides is possible due to its ability to exhibit a surface disorderliness. Considering the availability, suitability and wide application of Alumina in various applications, an effectively designed hybrid system of Alumina-based Nickel ferrite would be valuable towards possible application as antimicrobial or drug delivery agents to targeted organs in the human body system.

Various methods have been used previously for the synthesis of magnetic ferrites nanoparticles. Such methods include sol-gel

* Corresponding author.
E-mail address: k.ishaq@futminna.edu.ng (K. Ishaq).
Peer review under responsibility of Karabuk University.

http://dx.doi.org/10.1016/j.jestch.2016.12.008
2215-0986/

method, co-precipitation, thermolysis, combustion method, gel-assistant hydrothermal route, hydrothermal method, microemulsion, and precipitation ([7,2,6,10]. These methods of preparation pose the major challenge of particle agglomeration which subsequently limits their area of applications which necessitates the synthesis of the Alumina-based Nickel ferrite nanoparticles through wet impregnation method, which is a method known for its effectiveness and efficiency of product. Based on our knowledge, there are limited literature reports on the optimization of the synthesis of alumina-based nickel ferrites using central composite design (CCD) for biomedical application.

2. Methodology

The study seeks to address the synthesis, optimization and the potential application of the alumina-based nickel ferrite nanoparticles for its antibacterial effects on some selected microorganisms that are present in polluted water bodies. The Nickel nitrate hexahydrate, $Ni(NO_3)_2{\cdot}6H_2O$, iron nitrate nonahydrate $Fe(NO_3)_3{\cdot}9H_2O$, and α-alumina [Al_2O_3] were of analytical grade with percentage purity in the range of 98–99.99%. All chemicals were used without further purification.

2.1. Synthesis of $NiFe_2O_4$ doped α-alumina nanoparticles

Wet impregnation method was employed for the development of Nickel Ferrites nanoparticles on α-alumina. Solution of 0.0032 mol/dm^3 of $Fe(NO_3)_3{\cdot}9H_2O$ and 0.232 mol/dm^3 of $Ni(NO_3)_3{\cdot}6H_2O$ salts were impregnated with 7–8 g of α-alumina as support material to form an equal weight percent of Fe and Ni. The resulted mixture was allowed to age for 60 min under constant stirring at room temperature. The resulting homogeneous slurry was dried at a temperature of 110–115 °C for 6–8 h depending on the experimental run. The obtained product was grinded and calcined at 400 °C for 2 h. The calcined samples were allowed to cool and then sieved through 150 μm sieve size. Response surface methodology experimental design was used with Central Composite Design for the design of the experiments using Design Expert® version 7. Three experimental factors such as drying time (h), drying temperature (°C) and the weight of support material (g) were studied. This resulted in the generation of twenty (20) experimental runs. Table 1 shows the experimental ranges and levels of the factors used in the Central Composite Design while Table 2 depicts the experimental runs and the matrix for each runs.

The yields of the $NiFe_2O_4$ doped α-alumina nanoparticles were determined after the calcination of all samples at constant calcination temperature of 500 °C using the relationship presented in Eq. (1);

$$y\ (\%) = \frac{W_a - W_b}{W_a} \times 100 \quad (1)$$

where y is the yield (%), W_a is weight of sample before calcination (g) and W_b is the weight after calcination (g).

2.2. Characterization and ANOVA

2.2.1. Characterization of $NiFe_2O_4$ nanoparticles

The surface morphology and microstructure of the synthesised $NiFe_2O_4$ doped α-alumina nanoparticles were characterized using Zeiss Auriga HRSEM. The HRSEM equipped with EDS was used to determine the nickel-ferrite composition. A small quantity of the nickel ferrites was sprinkled and sputter coated with Au-Pd using Quorum T15OT for 5 min. The sputter coated samples was firmly attached to the carbon adhesive tape and analysed with In-lens standard detector at 30 kV electron high tensions (EHT) of 5 kV for imaging. The crystal phase identification of the powdered ferrites was performed using Bruker AXS D8 X-ray diffractometer system coupled with Cu-Kα radiation of 40 kV and a current of 40 mA.

Table 1
Levels of the factors considered in Central Composite Design.

Independent Variables	Coded symbols	−1 Level	+1 Level	−alpha	+alpha
Mass of support (g)	A	7	8	6.6591	8.3409
Drying Time (h)	B	6	8	5.31821	8.68179
Drying Temp. (°C)	C	110	115	108.296	116.704

Table 2
CCD Experimental matrix for the development of $NiFe_2O_4$ nanoparticles.

Run	Mass of Alumina (g)	Drying Time (h)	Drying Temp (°C)	Yield after Calcination (%)
1	8.00	6.00	115.00	87.87
2	7.00	8.00	110.00	89.87
3	7.00	6.00	110.00	76.76
4	7.50	7.00	112.50	70.99
5	8.00	8.00	110.00	70.90
6	7.50	7.00	112.50	89.90
7	7.00	8.00	115.00	91.09
8	8.00	6.00	110.00	92.87
9	7.50	7.00	112.50	77.90
10	7.00	6.00	115.00	78.98
11	7.50	7.00	112.50	84.59
12	8.00	8.00	115.00	78.89
13	7.50	8.68	112.50	69.97
14	7.50	5.32	112.50	88.88
15	7.50	7.00	108.30	78.96
16	7.50	7.00	112.50	87.98
17	7.50	7.00	116.70	97.45
18	6.66	7.00	112.50	96.77
19	8.34	7.00	112.50	87.87
20	7.50	7.00	112.50	78.98

The λ for Kα was 0.1541 nm, scanning rate was 1.5 °/min, while a step width of 0.05° was used over the 2θ range value of 20–80°.

2.2.2. Antibacterial activities

The antimicrobial activity of the developed nickel ferrite doped α-alumina nanoparticles was tested on three common bacteria pathogens, Gram-negative bacterium: *E. coli* and *Pseudomonas aeruginosa* and a Gram-positive bacterium *S. aureus*. The bacterial which were cultured on agar plates supplemented with varied concentration of nickel ferrite doped nanoparticles. The plates were incubated for 24 h at a temperature of 37 °C.

3. Results and discussion

This study is focus on the synthesis, characterization and antibacterial activities of Nickel ferrite doped α-alumina synthesised by wet impregnation method. The result presented in Table 2 represents the result obtained while studying the effect of synthesis parameters on the yield of nickel-ferrite doped alpha-alumina nanoparticles. Results as presented in Table 2 indicate that the highest yield of 97.45% was obtained at synthesis parameters of 6 h drying time, 7.50 g mass of alumina and 116.70 °C drying temperature. Results also revealed that combination of these parameters greatly influenced the nanoparticle yield. For instance, at constant mass of alumina of 8 g and drying time of 6 h, and varying the temperature from 110 °C to 115 °C, the obtained yield decrease from 92.89 to 87.87%. However, with the mass of alumina at 7 g, drying time of 8 h while the temperature was raised from 110 °C to 115 °C bring about increment in yield from 89.87 to 91.09%

The mathematical regression model generated via analysis of variance represented in terms of coded factors is presented in Eq. (2) which shows the interactive behaviours of the constituent factors on yield of the developed nickel-ferrite doped α-alumina.

$$\begin{aligned} Yield = {} & 82.26 - 2.65A - 5.62B + 5.50C - 7.02AB - 0.056AC \\ & + 1.50BC + 2.95A^2 - 1.61B^2 + 1.49C^2 + 1.75ABC \\ & + 4.91A^2B - 4.69A^2C + 1.87AB^2 \end{aligned} \quad (2)$$

where A is mass of alumina (g), B is the drying time (h), and C is the drying temperature (°C). The main effects in Eq. (2) revealed that the mass of alumina and the drying time have negative effects on the yield of nickel ferrite nanoparticles, while the drying tempera-

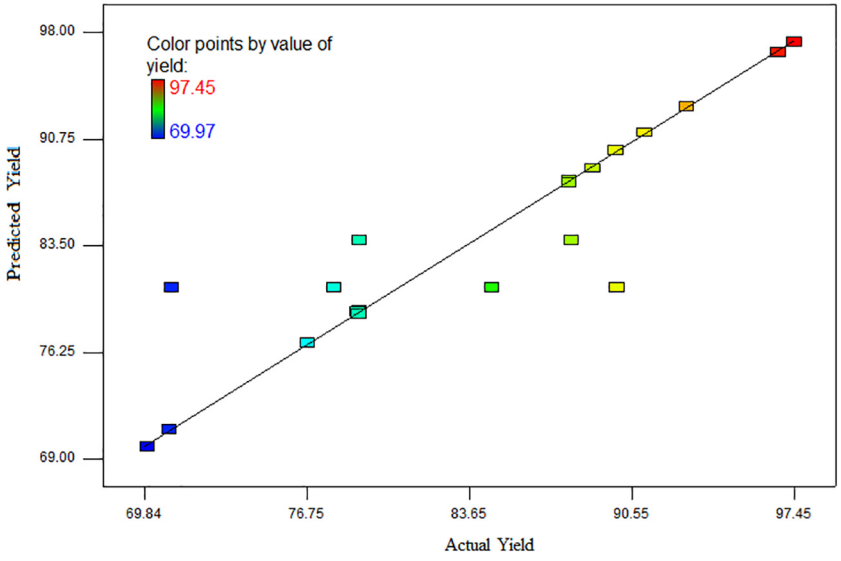

Fig. 1. Correlation between the predicted and actual yields.

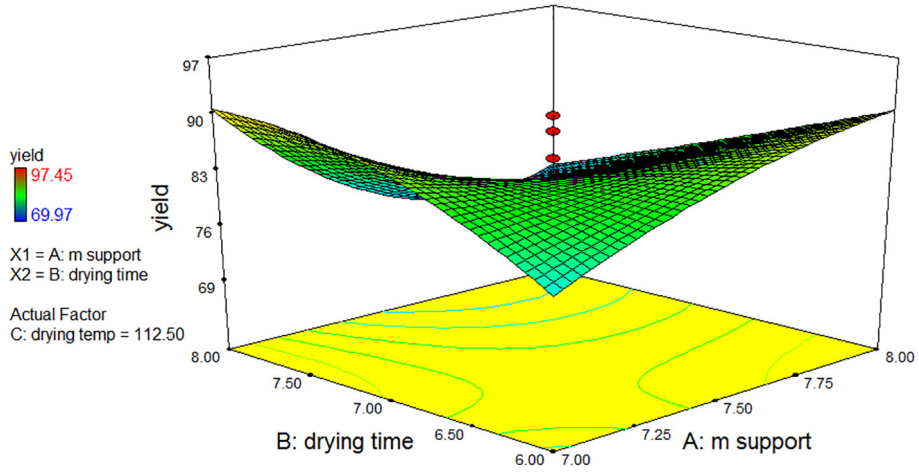

Fig. 2a. Response surface plot showing the relationship between drying time and mass of support on the yield nickel-ferrite doped alumina.

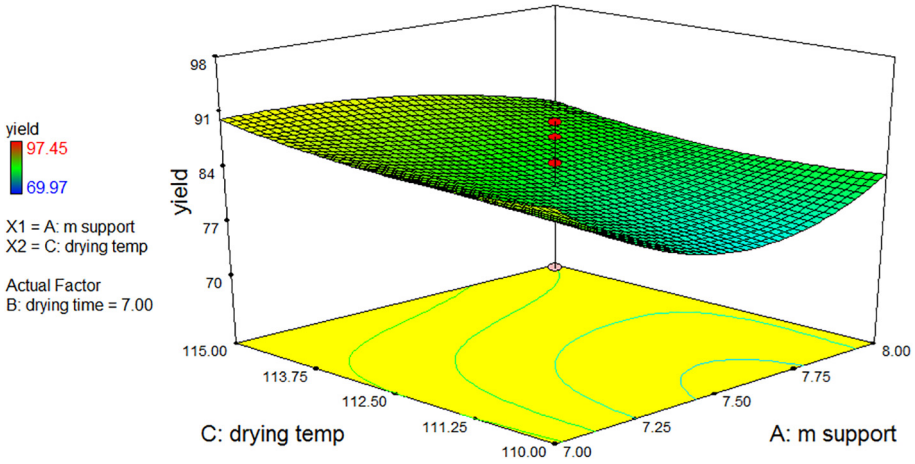

Fig. 2b. Response surface plot showing the relationship between drying temperature and mass of support on the yield nickel-ferrite doped alumina.

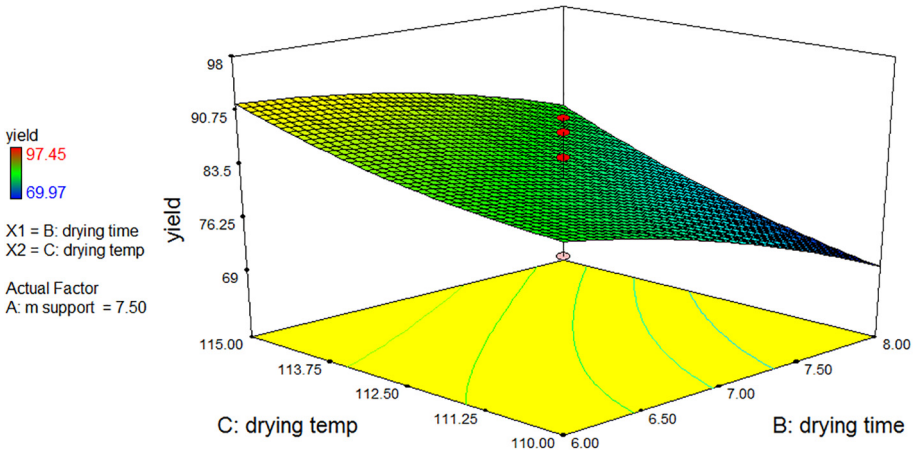

Fig. 2c. Response surface plot showing the relationship between drying temperature and drying time on the yield nickel-ferrite doped alumina.

ture influences the yield positively. The model R^2 value of 0.8115 and a correlation coefficient of 0.9999 between the predicted and actual yields indicate that the model is reliable, and this is further supported by Fig. 1.

The p-values less than 0.0500 which is equivalent to 95% confidence level indicates that model terms are significant. Consequently, only the two-way interaction between the mass of alumina and the drying duration were significant model terms. A predicted R^2 of 0.3495 was obtained which is in reasonable agreement with the adjusted R^2 of 0.3214. The signal to noise ratio of 4.553 was an adequate signal being greater than 4. Thus, the model can be used to navigate the design space. Fig. 2a–2c presents the 3D surface response plots which show the two-way interactive effects of the three factors considered.

3.1. Characterization of $NiFe_2O_3$ nanoparticles

The surface morphology of the developed Nickel Ferrites nanoparticles was determined via Scanning electron microscope (SEM). The result of the SEM micrographs of experimental run with the highest yield is presented in Fig. 3.

The SEM micrograph as depicted in Fig. 3 shows the extent of effective dispersion of Nickel-ferrites on the surface of the alumina. This shows that the adopted wet impregnation method aids in effective dispersion of the Nickel ferrites on the precursor therefore giving rise to maximum surface contact of the ferrite to any reaction environment. The elemental composition of the nickel-ferrites was further analysed using the EDS. The result of the analysis is as shown in Fig. 4a.

The main constituent of the magnetic based nanoparticles were observed to be C, O, Al, Fe and Ni with 74.79, 14.8, 8.37, 1.12 and

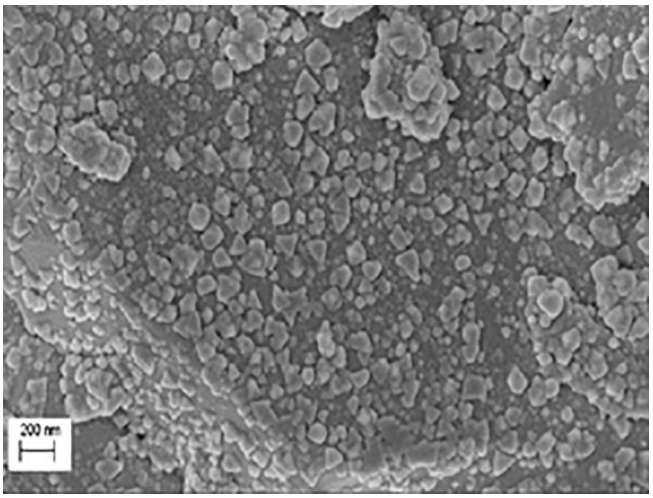

Fig. 3. SEM of the developed $NiFe_2O_4$ Nanopowder (Highest-yield sample).

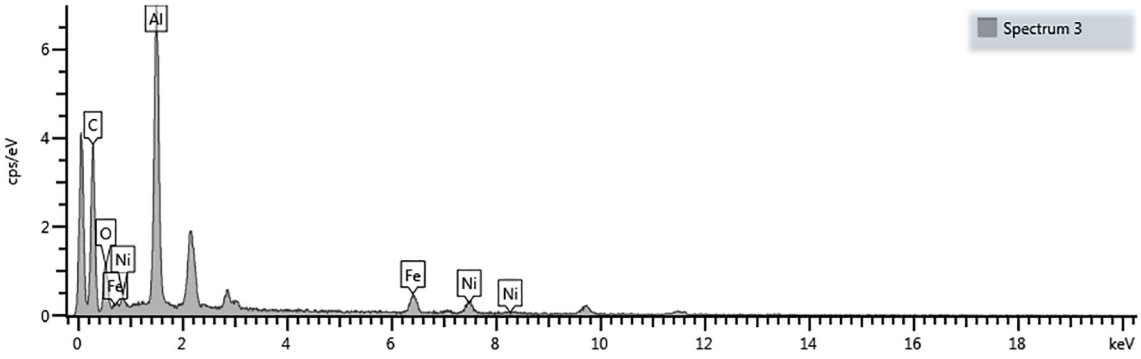

Fig. 4a. EDS spectrum of nickel ferrite (Highest-yield sample).

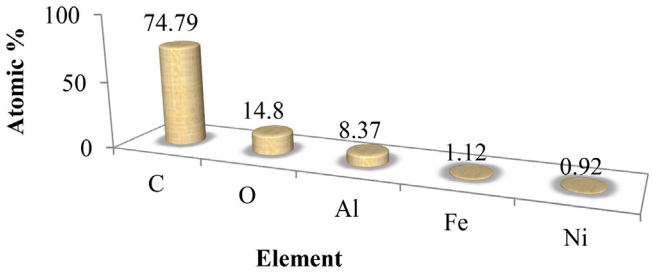

Fig. 4b. Elemental composition of nickel ferrite (Highest-yield sample).

0.92% respectively as shown in Fig. 4b. High carbon content depicted in the compositional mix is as a result of the carbon grid used during the process of SEM/EDS analysis while oxygen was resulted from the formation of oxides composition in the form of magnetic ferrites ($NiFe_2O_4$) which was successfully doped onto the alumina precursor.

The crystallinity of the synthesised $NiFe_2O_4$ doped on alumina was characterized via the XRD technique. The result of the analysis is presented in Fig. 5 (where A-T represent run 1–20) following the format represented in Table 2. The crystallography of the $NiFe_2O_4$ doped alumina practically has similar characteristics at the same

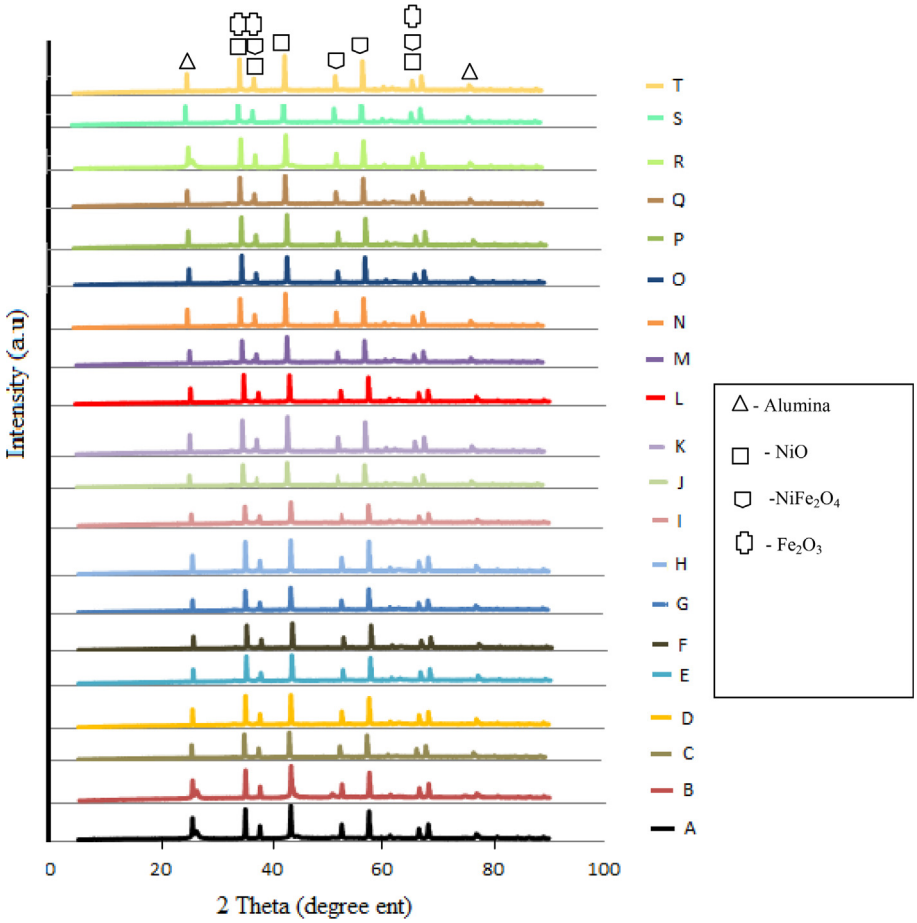

Fig. 5. XRD of the developed nickel ferrites via CCD.

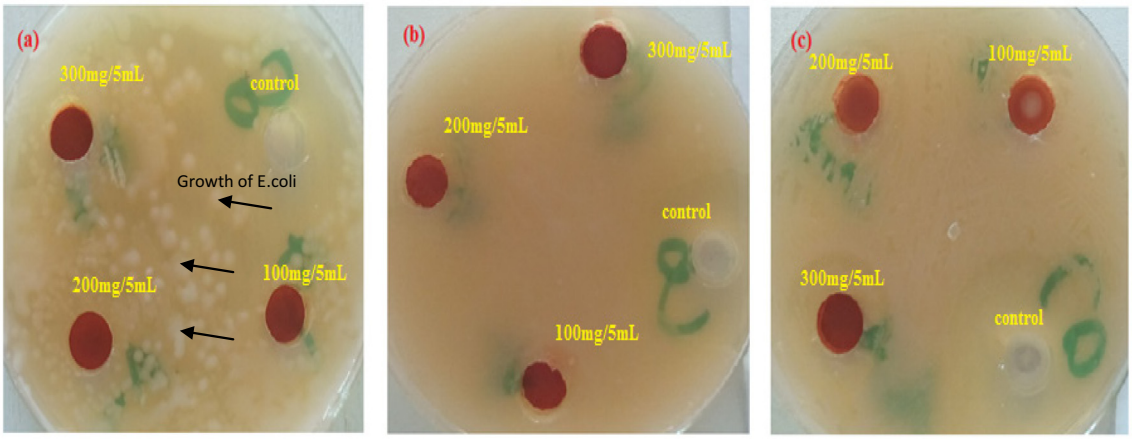

Plate 1. Antibacterial activity of Nickel ferrites on (a) E. coli (b) Pseudomonas aeruginosa and (c) Staphylococcus aureus.

diffraction angle. Basically, the diffraction angle at 2θ equal 23.50 and 78.11 are attributed to the alumina precursor. The presence of NiO and Fe_2O_3 were as a result of the interaction of nickel and iron with air during the calcination process respectively. The formation of NiO was observed at the diffraction angle of 36.10, 38.61 and 42.72° while the presence of Fe_2O_3 was observed at diffraction angle of 36.10, 38.61 and 68.91°. The diffraction peaks around 52.93, 59.45, 68.12 and 68.91 are attributed to the formation $NiFe_2O_4$ on the alumina precursor.

3.2. Antibacterial activities of nickel ferrite nanoparticles

The antibacterial activities of the developed Nickel ferrite Nanopowder was tested on the selected microbes: *Escherichia coli*, *Pseudomonas aeruginosa* and *Staphylococcus aureus*. Agar well diffusion method was employed for the antimicrobial activity of the nickel ferrite doped alumina. The choice of the bacterium was based on the common infection affecting the community resulted from their intakes when present in polluted water. For instance, the presence of E. coli DO17 causes nausea, diarrhoea while whooping cough in both children and adults is caused by a very pathogenic microbe called Pseudomonas aeruginosa. Meanwhile, the effect of *Staphylococcus aureus* is noticeable and also a causative bacterial in boil and causes complication in wounds. With the possible presence of these dangerous bacterium in water, there is need to effectively develop a nano-based antibacterial inhibitors to mitigate their growth and functionality in water system. To determine the efficient and the best dosage loading for the best antibacterial activity, the ratio of mass of dosage of the nickel ferrites to the solvent (DMSO) was varied. The results of the antibacterial activities were presented in the form of area of inhibition as shown in Plate 1 while the diameter of inhibition is shown in Table 3.

From Table 3, the nickel ferrites nanoparticles possess no antibacterial activity on the E. coli microbes but show a more observable effect on the *Pseudomonas aeruginosa* and *Staphylococcus aureus* except in 100 mg/mL in *Pseudomonas aeruginosa.* The antibacterial effects observed in *Staphylococcus aureus* and *Staphylococcus aureus* were as a result of the ability of nickel ferrites to induce gaps and pits which causes the membrane of the bacterium cells to fragment. The results as presented in Table 3 further shows that as the ferrites loading increases, the antibacterial effect on *Pseudomonas aeruginosa* increases with inhibition diameter from 0 to 13 and then to 17 mm for 100 mg, 200 mg and then 300 mg of nickel ferrites loading respectively. Considering the effect of nickel ferrites on *Staphylococcus aureus*, there was progressive increase in inhibition growth of 100–200 mg loading from 0.70 to 1.20 respectively. Further increase in ferrites dosage does not pose any inhibitory characteristics to the *Staphylococcus aureus*. This mechanism of cell fragmentation has also been observed in the work of Amro et al. [1] and Hyosuk et al. [3] who reported on the effect of CNT-Ag and GO-Ag nanocomposites against Gram-negative and Gram-positive Bacteria. This excellent antibacterial property possesses by the developed nickel ferrites nanoparticles on *Staphylococcus aureus* and *Pseudomonas aeruginosa* makes it good source of disinfectant in polluted water body with effective properties that enhance microbe inhibition.

Table 3
Zone of inhibition (mm) of the nickel ferrite loading on waterborne microbes.

Bacterial	Zone of inhibition (mm)		
	100 mg/5 ml DMSO	200 mg/5 ml DMSO	300 mg/5 ml DMSO
E. coli	–	–	–
Pseudomonas aeruginosa	–	13.00	17.00
Staphylococcus aureus	0.70	1.20	1.20

4. Conclusion

The possible synthesis of highly functional nickel ferrites doped α-alumina for antibacterial activities has been observed via central composite design (CCD) using wet impregnation method. The wet impregnation method depicts effective dispersion of doped ferrites on the precursor material during the calcination process. The developed $NiFe_2O_4$ doped alumina was characterized via SEM, EDS and XRD to determine its morphology, elemental composition and crystalline mix. The highest ferrite's yield was further applied as an antibacterial on three selected microorganisms in waterbody and their effectiveness regarding the dosage loading was during inoculation process. The nickel ferrites show the highest inhibitory effect on *Pseudomonas aeruginosa* at the dosage of 300 mg/mL of DMSO with no effect on E. coli.

Acknowledgments

Authors appreciate the financial assistance received from TETFund Nigeria under the grant number TETF/DESS/FUTM2016/STI/Vol 1 and also the Centre for Genetic Engineering and Biotechnology, FUT Minna, Nigeria for using their facilities.

References

[1] N.A. Amro, L.P. Kotra, K. Wadu-Mesthrige, A. Bulychev, S. Mobashery, G.Y. Liu, High-resolution atomic force microscopy studies of the Escherichia coli outer membrane: structural basis for permeability, Langmuir 16 (6) (2000) 2789–2796.

[2] L. Gup, X. Shen, X. Meng, Y. Feng, Effect of Sm 3^{+} ions doping on structure and magnetic properties of nanocrystalline $NiFe_2O_4$ fibers, J. Alloys Compd. 490 (1) (2010) 301–306.

[3] Y. Hyosuk, D.K. Ji, C.C. Hyun, W.L. Chul, Antibacterial activity of CNT-Ag and GO-Ag nanocomposites against Gram-negative and Gram-positive bacteria, Bull. Korean Chem. Soc. 34 (11) (2013) 3261–3264.

[4] I. Kariim, A.S. Abdulkareem, O.K. Abubakre, I.A. Mohammed, M.T. Bankole, T.O. Jimoh, Studies on the suitability of alumina as bimetallic catalyst support for MWCNTs growth in a CVD reactor, International Engineering Conference (IEC 2015).

[5] S.D. Mathew, R.S. Juang, An overview of the structure and magnetism of spinel ferrite nanoparticles and their synthesis in microemulsions, Chem. Eng. J. 129 (2007) 51–65.

[6] S.M. Patange, S.E. Shirsath, S.S. Jadhav, K.S. Lohar, D.R. Mane, K.M. Jadhav, Rietveld refinement and switching properties of Cr^{3+} substituted $NiFe_2O_4$ ferrites, Mater. Lett. 64 (6) (2010) 722–724.

[7] M.K. Shobana, S. Sankar, Structural, thermal and magnetic properties of $Ni_{1-x}Mn_xFe_2O_4$ nanoferrites, J. Magn. Magn. Mater. 321 (2009) 2125–2128.

[8] R. Suresh, P. Moganavally, M. Deepa, Synthesis and characterization of nickel ferrites nanoparticles, Int. J. ChemTech Res. 8 (5) (2015) 113–116.

[9] J. Wang, C. Zeng, Z. Peng, Q. Chen, Synthesis and magnetic properties of $Zn_{1-x}Mn_xFe_2O_4$ nanoparticles, Phys. B 349 (2004) 124–128.

[10] J. Zhu, D. Xiao, J. Li, X. Yang, Y. Wu, Characterization of FeNi3 alloy in Fe–Ni–O system synthesized by citric acid combustion method, Scr. Mater. 54 (2006) 109–113.